Journal of Inflammation Research

Dovepress
Taylor & Francis Group

Open Access Full Text Article

ORIGINAL RESEARCH

Aggregation of Stress Granules Induced by Hypoxia and Lipopolysaccharide via PKR-p-eIF2α Pathway and 4EBP1 Pathway Inhibits the Inflammatory Response in Peri-Implantitis

Shuang Li[1,2,*], Chunling Ma[3,*], Chun Fan[4], Yanshan Liu[5], Jian Li[2,6], Baoheng Yin[1,2], Lingmei Zhong[7], Na Bai[1,2], Zhiyuan Li[3]

[1]Department of Prosthodontics, The Affiliated Hospital of Qingdao University, Qingdao, Shandong, People's Republic of China; [2]School of Stomatology, Qingdao University, Qingdao, Shandong, People's Republic of China; [3]Medical Research Center, The Affiliated Hospital of Qingdao University, Qingdao, Shandong, People's Republic of China; [4]Department of Periodontology, The Affiliated Hospital of Qingdao University, Qingdao, Shandong, People's Republic of China; [5]Department of Maxillofacial Surgery, The Affiliated Hospital of Qingdao University, Qingdao, Shandong, People's Republic of China; [6]Department of Oral Implantology, The Affiliated Hospital of Qingdao University, Qingdao, Shandong, People's Republic of China; [7]Department of Pulmonary and Critical Care Medicine, The Affiliated Hospital of Qingdao University, Qingdao, Shandong, People's Republic of China

*These authors contributed equally to this work

Correspondence: Zhiyuan Li; Na Bai, Email zyli0120@163.com; na.bai@qdu.edu.cn

Objective: To investigate whether stress granules (SGs) exist in peri-implantitis (PI) and to explore the formation mechanism and role of SGs in the response of human gingival fibroblasts (hGFs) to hypoxia or LPS.

Methods: Gingival tissues were collected from patients with PI and from healthy individuals. RT-qPCR, Western blotting, and immunofluorescence staining were used to detect the SGs in the gingiva. Healthy hGFs were cultured and the activation of SGs in LPS- or hypoxia-treated hGFs was evaluated. Knockdown assays using siRNAs were performed to investigate the formation mechanism and the role of SGs in hGFs.

Results: SGs aggregates were present in gingival tissues of patients with PI. LPS or hypoxia stimulation induces SGs formation and leads to eIF2α phosphorylation and 4EBP1 hypophosphorylation in hGFs. Knockdown of PKR or 4EBP1 decreases the number of SGs in stressed hGFs and enhances LPS- and hypoxia-induced TNF-α and IL-1β expression.

Conclusion: Our study revealed SGs aggregation in the PI gingiva. Hypoxia and LPS can induce SGs assembly in hGFs in vitro via PKR-p-eIF2α and 4EBP1 pathways. SGs in hGFs exert a protective effect against inflammatory responses, suggesting their role in balancing pro- and anti-inflammatory responses, thus providing a new approach for protecting against destructive inflammatory responses.

Plain Language Summary: Hypoxia and *Porphyromonas gingivalis*-LPS induced SGs assembly in hGFs via the PKR-p-eIF2α and 4EBP1 pathways, whereas SGs exerted a protective effect against hypoxia and *P. gingivalis*-LPS-induced inflammatory response.

Keywords: peri-implantitis, stress granules, hypoxia, LPS

Introduction

Peri-implantitis (PI) is a pathological state that manifests as an inflammatory response within the soft tissues surrounding the implant, and is accompanied by progressive loss of bone tissue, which is the main cause of dental implant failure.[1] The primary causes of PI are immunological responses to microbial infections, which are caused by gram-negative bacteria, particularly *Porphyromonas gingivalis*.[2,3] Periodontopathic bacteria produce various virulence factors including lipopolysaccharide (LPS) and peptidoglycan.[3] Human gingival fibroblasts (hGFs) are the most abundant structural cells

Received: 19 February 2025
Accepted: 26 July 2025
Published: 4 August 2025

Graphical Abstract

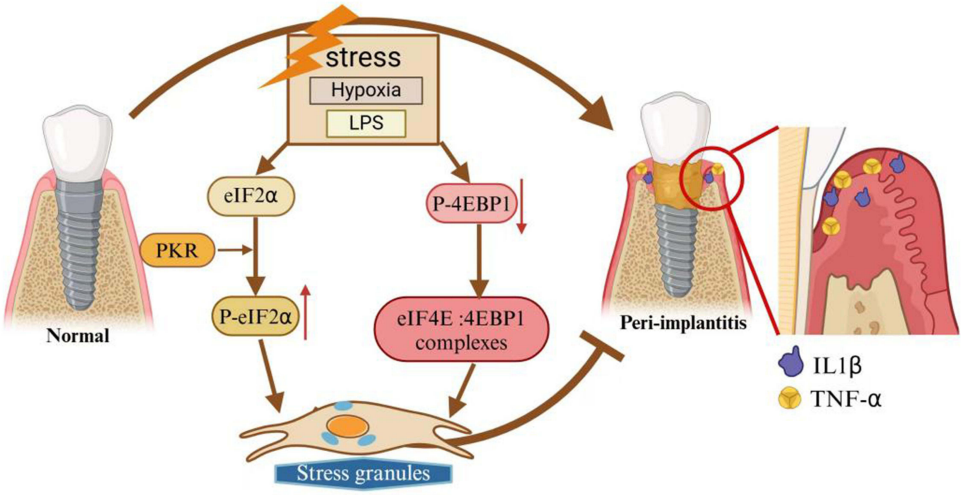

in periodontal tissue and are capable of releasing IL-6, IL-1β, and TNF-α after *P. gingivalis*-LPS stimulation.[4–6] Hypoxia and inflammation have a close causal relationship, as hypoxia can trigger inflammatory responses and inflammatory lesions are often accompanied by hypoxic tissue changes.[7,8] Peri-implant tissues are more vulnerable to hypoxia and inflammation than natural teeth because of the absence of cellular and vascular structures as well as linking epithelial and periodontal membranes.[9] A hypoxic environment exists around the implant in the PI.[7,10] Further research into the regulatory mechanisms underlying hypoxia and inflammation will contribute to the treatment of PI.

Stress granules (SGs) are formed under stress conditions such as heat shock, ischemia, hypoxia, or microbial infection.[11] SGs are intricate and mutable nonmembrane-bound cellular structures that are composed of untranslated mRNA and a spectrum of proteins.[12] They serve as regulatory centers that govern translation, ribosome homeostasis, and protein homeostasis and function as signaling hubs that influence cell survival and the ability to recover from stress.[13] Recent studies have established a strong link between SG formation and development of inflammatory conditions.[14,15] Within eukaryotic cells, canonical formation of stress granules commences with phosphorylation of the eIF2α subunit by specific kinases such as PKR, GCN2, HRI, or PERK. Consequently, eIF2α phosphorylation results in the aggregation of mRNAs and proteins involved in translation, ultimately forming SGs.[16,17] Under certain stress conditions, the accumulation of unphosphorylated 4EBP1 within the cell, which impedes the initiation of translation, can also lead to SGs formation.[18] The pathways associated with SGs formation and function are increasingly recognized as promising targets for therapeutic strategies in a variety of diseases.[19–22]

However, to date, SGs have not been reported in the PI. This study is the first to investigate whether SGs exist in the gingiva of PI, and to explore the formation mechanism and role of SGs in the production of inflammatory mediators in hGFs under hypoxia or *P. gingivalis*-LPS stimulation.

Materials and Methods

Human Gingival Tissue Collection

PI was diagnosed based on the criteria reported previously.[23] The PI group had a probing depth > 5 mm and marginal bleeding at least one implant site, and bone loss. Patients with PI were recruited from the Department of Stomatology of the Affiliated Hospital of Qingdao University between June 2022 and June 2024. The PI gingival tissues (n=15) were obtained from the extracted peri-implant with advanced alveolar bone destruction. Gingival tissues (n=15) obtained from the third molars of healthy patients who underwent dental surgery were used as healthy controls. Exclusion criteria were systemic inflammatory diseases or conditions, pregnancy or breastfeeding, missing multiple teeth (10 or more), drug use,

smoking, previous antibiotic use, or periodontal treatment within six months. Ethical approval for this study was granted by the Institutional Review Board (IRB) of the Affiliated Hospital of Qingdao University (IRB no. QYFYWZLL29422), and informed consent was obtained from all participants in accordance with the Declaration of Helsinki. The demographic and clinical data of the patients are shown in Table 1.

hGFs Culture and Treatment

Epithelial tissues of excised healthy gingiva were removed, and the remaining tissues were cut into small blocks (approximately 1–3 mm^2) and inoculated at the bottom of the T25 flasks. α-MEM containing 20% fetal bovine serum (Biological Industries, Kibbutz, Israel) was added to T25 flasks. The tissue fragments were cultured at 37°C and 5% CO_2 for 7–10 days, and hGFs migrated out from the edges. The hGFs were passaged and cultured in α-MEM containing 10% FBS and 1% penicillin-streptomycin (Solarbio, China). hGFs between passages 3 and 7 were used in the experiments.

For stress stimulation, 2×10^5 hGFs seeded in 12-well plates were treated with *P. gingivalis* LPS (1μg/mL; InvivoGen) or hypoxia for 24 h. Hypoxia was induced by placing the cells in a hypoxic incubator (94% N_2, 5% CO_2, and 1% O_2; Baker Ruskinn).

RT-qPCR

Total RNA was extracted from gingival tissues or hGFs using the RNA-easy reagent (Vazyme) and then reverse-transcribed using the PrimeScript RT Reagent Kit (Vazyme). qPCR amplification was performed using SYBR GREEN mix (TAKARA). The primers used are listed in Table 2.

Western Blotting

For total protein extract, gingival tissues and hGFs were lysed using 2% sodium dodecyl sulfate (SDS) lysis buffer (Biyuntian Biotechnology).

For soluble-insoluble fractionation of lysates, hGFs were lysed in ice cold polysome buffer (20 mM Tris-HCl pH 7.4, 1.25 mM $MgCl_2$, 100 mM KCL, 0.5% NP-40 + PMSF),[24] incubated on ice for 10 min, and passed through a hypodermic needle 10 times. Then the lysates were clarified by centrifugation at 4 °C, 12000 g for 15 min to separate the soluble fraction. The soluble fraction was removed and mixed with one volume of 2 x Laemmli loading buffer. The pellet was dissolved in PBS and mixed with 2 x Laemmli loading buffer forming the insoluble fraction.

The primary antibodies used for incubation with PVDF membranes (Millipore) were anti-HuR (Abcam), anti-eIF2α (CST), anti-4EBP1 (CST), anti-p-IRE1 (Abcam), anti-p-eIF2α (CST), anti-p-4EBP1 (CST), anti-β-tubulin (Abcam), anti-G3BP (Abcam), anti-TRAF2 (Selleck). After washing, the membranes were incubated with horseradish peroxidase (HRP)-labeled secondary antibodies (Biyuntian Biotechnology). The protein bands were detected using a chemiluminescent HRP substrate (Millipore) and analyzed using ImageJ software.

Table 1 Demographic and Clinical Characteristics of Peri-Implantitis Patients

	Peri-Implantitis (n = 15)	**Healthy Controls (n = 15)**
Age (years)	48.73 ± 11.67	50.27 ± 14.73
Gender (M:F)	9:6	10:5
Probing depth (mm)	5.93±0.56*	1.97±0.69
Bone loss >3 mm (%)	93.33	0

Notes: Data are presented as mean ± standard deviation. *$P < 0.05$ vs healthy controls, Wilcoxon rank-sum test.

https://doi.org/10.2147/JIR.S523799

Table 2 Primers Used for RT-qPCR

Gene Name	Orientation	Primer Sequence (5' – 3')
GAPDH	Forward	CATGTTCGTCATGGGTGTGAA
	Reverse	GGCATGGACTGTGGTCATGAG
IL-1β	Forward	CTGAGCACCTTCTTTCCCTTCA
	Reverse	TGGACCAGACATCACCAAGCT
TNF-α	Forward	TGTAGCCCATGTTGTAGCAAACC
	Reverse	GAGGACCTGGGAGTAGATGAGGTA
DDX6	Forward	GAAATGGCTTATGCCGCAAT
	Reverse	GATGACCAAAGCGACCTGATC
FUBP1	Forward	GGAATGGTTGGATTCATAATTGG
	Reverse	CTGACTGGACAGATTCAGGTGTTC
ELAVL1	Forward	GAGGTGATCAAAGACGCCAACT
	Reverse	CGCAACCCCTCTGGACAA
AGO1	Forward	GCCTATGTTCCGGCATCTCA
	Reverse	ACGTTCTTCACCTGCACACACT
LSM4	Forward	GTTGGTGGAGCTGAAAAATGG
	Reverse	GGCATCCGCCAGAACTTGT
FTO	Forward	TCACAACCTCGGTTTAGTTCCA
	Reverse	TGCAGGCTCAAAGGATTTCA
METTL3	Forward	ATCGACCCTGTCGCAAGCT
	Reverse	CCTCAGAATCCATGCAAGCA

Transfection

hGFs grown to 80–90% confluence were transfected with the indicated siRNAs (Table 3, GeneChem, Shanghai, China) using Lipofectamine 3000 (Thermo Fisher Scientific). After 24 h of transfection, hGFs were treated with *P. gingivalis* LPS (1μg/mL) and hypoxia (1% O_2).

Immunofluorescence Assay

Tissue-Tek OCT (Sakura Finetek, CA, USA)-embedded gingival samples were sectioned into 6 μm sections. The sections or hGFs were fixed with 4% paraformaldehyde solution for 20 min, permeabilized with 0.1% Triton-X 100 for 15 min, and blocked with 5% bovine serum albumin at room temperature for 1 h before incubation with primary antibodies anti-HuR (Abcam), anti-G3BP (Abcam) or anti-TRAF2 (Selleck) at 4°C overnight. After incubation, the

Table 3 siRNAs Used for Transfection

siRNA name	Orientation	Sequence (5' - 3')
Con-siRNA	Forward	UUCUCCGAACGUGUCACGUTT
	Reverse	ACGUGACACGUUCGGAGAATT
PERK-siRNA	Forward	GCAGUCAUCAGUCAGAAUUTT
	Reverse	AAUUCUGACUGAUGACUGCTT
PKR-siRNA	Forward	CCUGAGACCAGUGAUGAUUTT
	Reverse	AAUCAUCACUGGUCUCAGGTT
4EBP1-siRNA	Forward	UCCUGAUGGAGUGUCGGAATT
	Reverse	UUCCGACACUCCAUCAGGATT
GCN2-siRNA	Forward	GCACUUUACGAGACACCAUTT
	Reverse	AUGGUGUCUCGUAAAGUGCTT
HRI-siRNA	Forward	CCAAGUAUAUCCAGCACUUTT
	Reverse	AAGUGGUGGAUAUACUUGGTT

sections or hGFs were incubated with fluorescently labeled secondary antibodies (Abcam). After staining with DAPI, images were captured using a fluorescent microscope (Thermo Fisher Scientific).

Histopathology

Gingival tissues were fixed in 10% formalin, embedded in paraffin, sectioned into 4 μm sections, and stained with hematoxylin and eosin (H&E).

ELISA Assay

TNF-α and IL-1β levels in the hGF supernatants were measured using commercially available ELISA kits (Elabscience).

Statistical Analysis

Data are presented as mean ± standard deviation. Data were analyzed using GraphPad Prism software. The Student's *t*-test was used for comparisons between two groups. When comparing multiple groups, one-way ANOVA with Tukey's multiple comparison test was performed. A *P*-value of <0.05 indicated statistical significance.

Results

The age and sex of the participants were similar ($P>0.05$). Probing depth values of the healthy controls were lower than those of the PI groups ($P<0.05$) (Table 1).

Histological Assessment

The radiographic results showed significant bone resorption around the dental implants in the patient with PI, and the white line of the bone at the apex of the alveolar ridge was not visible (Figure 1A). H&E staining was used to analyze the

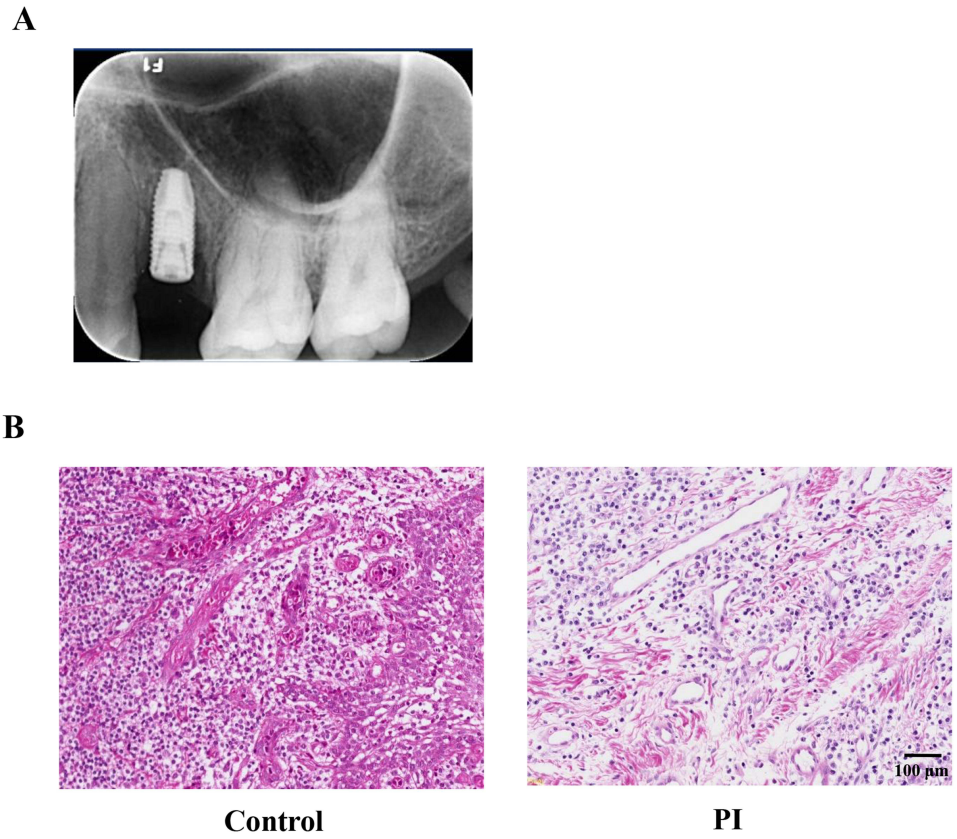

Figure 1 Histopathological images (**A**) Radiographic examination of a patient with PI. (**B**) H&E-stained images of gingival tissues from healthy controls or patients with PI (n=6). Scale bar 100 μm.

https://doi.org/10.2147/JIR.S523799

pathological features of the gingival samples. The healthy gingiva had a normal morphology, with a large number of fibroblasts and well-arranged collagen fiber bundles. In the gingiva of patients with PI, there were decreased fibroblasts, disruption of collagen fiber bundles, and lymphocytic infiltration in the underlying connective tissue around the dilated capillaries (Figure 1B).

SGs Aggregation in PI Gingiva

SGs play an important role in regulating inflammatory responses. We first analyzed the expression of SG-related genes using qPCR and found that the expression of genes such as *AGO1, ELAVL1, LSM4, DDX6*, and *FUBP1* was increased in PI gingival tissues (Figure 2A). We further analyzed the expression of two SGs marker proteins, HuR and G3BP, by Western blotting, which showed that the protein levels of HuR and G3BP were significantly elevated in the PI gingival tissues significantly (Figure 2B and C). To confirm whether SGs aggregated in PI, we co-localized HuR and G3BP by immunofluorescence staining and showed obvious SGs aggregation in PI gingival tissues but rarely in normal gingival tissues (Figure 2D and E).

P. gingivalis-LPS or Hypoxia Induces SGs Aggregation in hGFs

A hypoxic microenvironment exists in PI.[7,10] The parthenogenetic anaerobic bacterium *P. gingivalis* is the dominant bacterium in peri-implantitis and *P. gingivalis*-LPS is involved in the pathogenesis of PI. To investigate the mechanism of SGs aggregation in PI, we isolated hGFs from healthy gingival tissues and cultured them with *P. gingivalis*-LPS or 1% O_2 in vitro. As shown in Figure 3A, most hGFs exhibited fibroblast spindle morphology, and primary cells cultured for generations 3–7 were selected for subsequent experiments. qPCR results showed that *P. gingivalis*-LPS or 1% O_2 stimulation upregulated the expression of many SG-related genes in hGFs (Figure 3B). Western blot analysis revealed that *P. gingivalis*-LPS or 1% O_2 significantly upregulated the expression of HuR and G3BP and the phosphorylation level of the endoplasmic reticulum stress-sensing molecule IRE1 in hGFs (Figure 3C and D). We further determined whether *P. gingivalis*-LPS or 1% O_2 could induce SGs aggregation using an immunofluorescence assay. Compared to the control, *P. gingivalis*-LPS or 1% O_2 treatment induced SG formation, and the combination of *P. gingivalis*-LPS and 1% O_2 treatment was more significant (Figure 4).

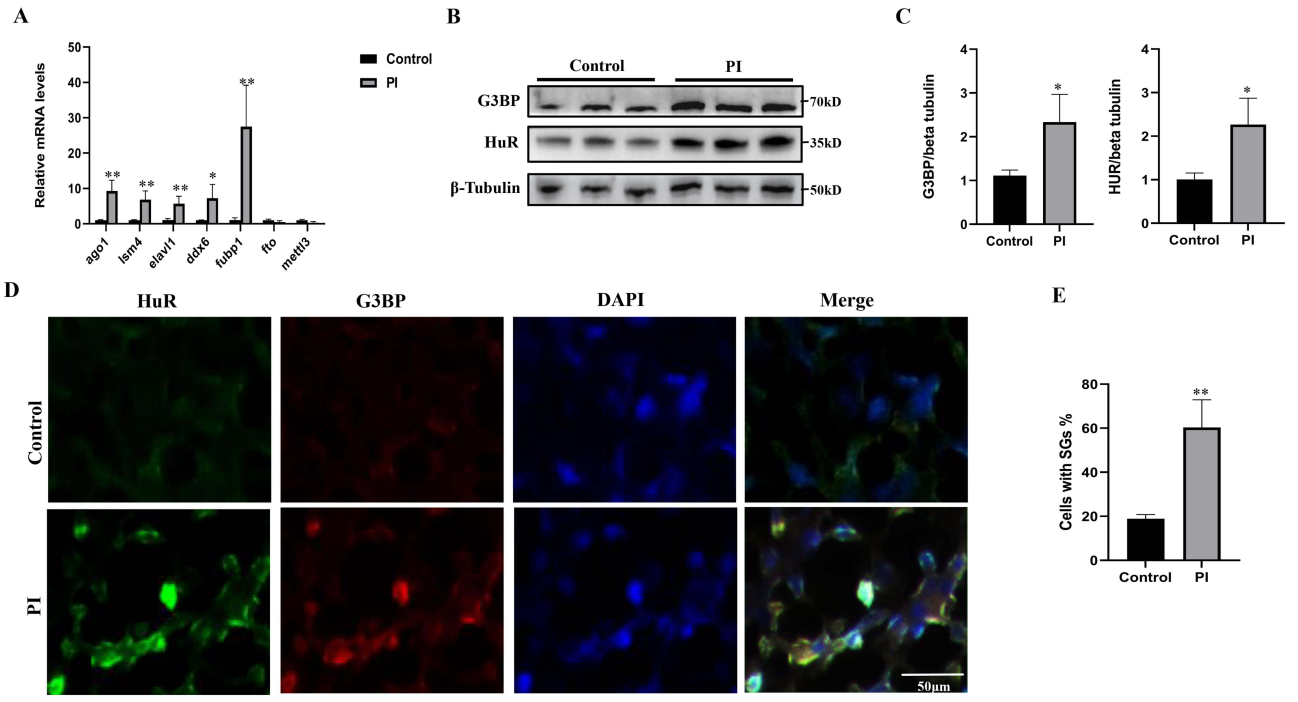

Figure 2 Assembly of stress granules in gingiva of PI (**A**) qPCR analysis of SG-related genes *AGO1*, *ELAVL1*, *FUBP1*, *FTO*, *METTL3*, *DDX6*, and *LSM4* in the gingival tissues (n=8). (**B** and **C**) Western blot analysis of G3BP and HuR protein levels in the gingival tissues of PI (n=6). (**D** and **E**) Immunofluorescence staining of G3BP and HuR proteins in gingival tissues in situ (n=6), scale bar: 50 μm. *$P < 0.05$, **$P < 0.01$ vs Control.

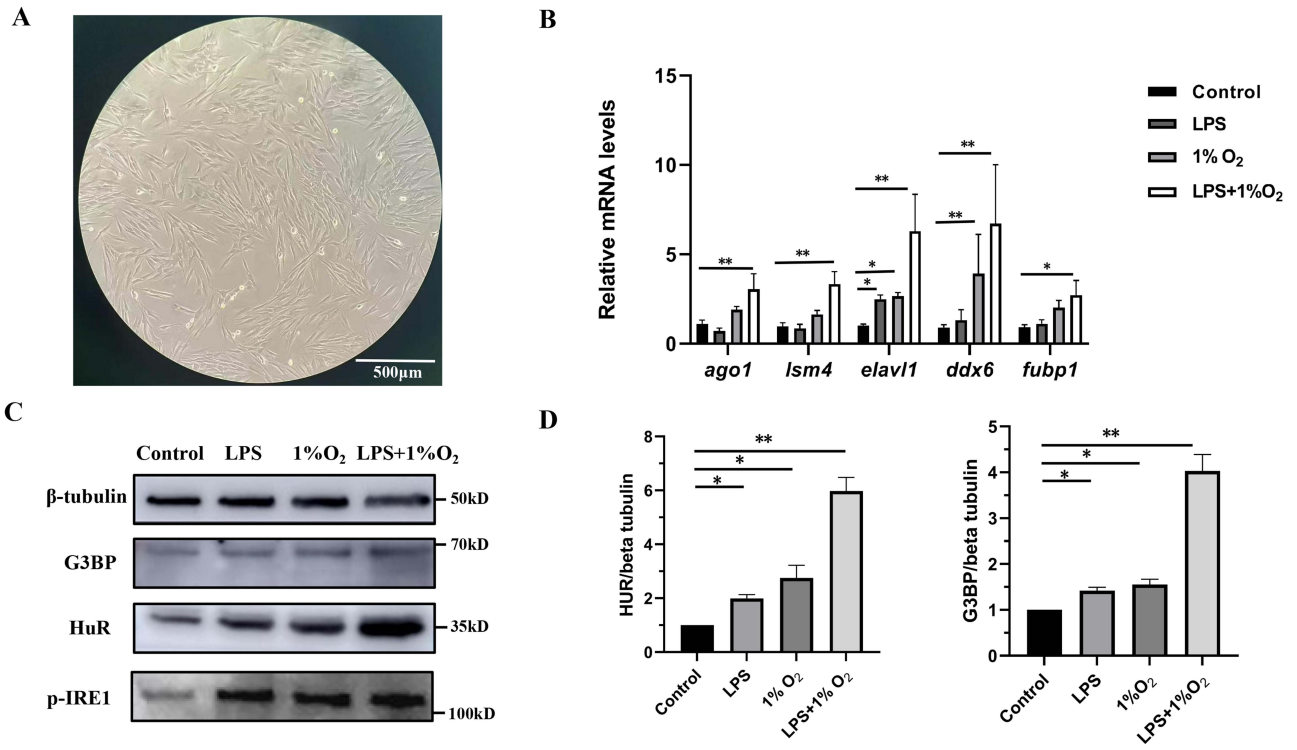

Figure 3 *P. gingivalis*-LPS or 1% O_2 induce stress response in hGFs (**A**) Images of primary cultured hGFs. Scale bar 500 μm. (**B**) qPCR analysis of SG-related genes *AGO1*, *ELAVL1*, *FUBP1*, *DDX6*, and *LSM4* levels in hGFs treated with *P. gingivalis*-LPS (1 μg/mL) or 1% O_2 for 24 h. (**C and D**) Western blot analysis of G3BP, HuR, and p-IRE1 protein levels in hGFs treated with *P. gingivalis*-LPS (1 μg/mL) or 1% O_2 for 24 h. **P* <0.05, ***P*<0.01, vs Control. Data are representative of three independent experiments.

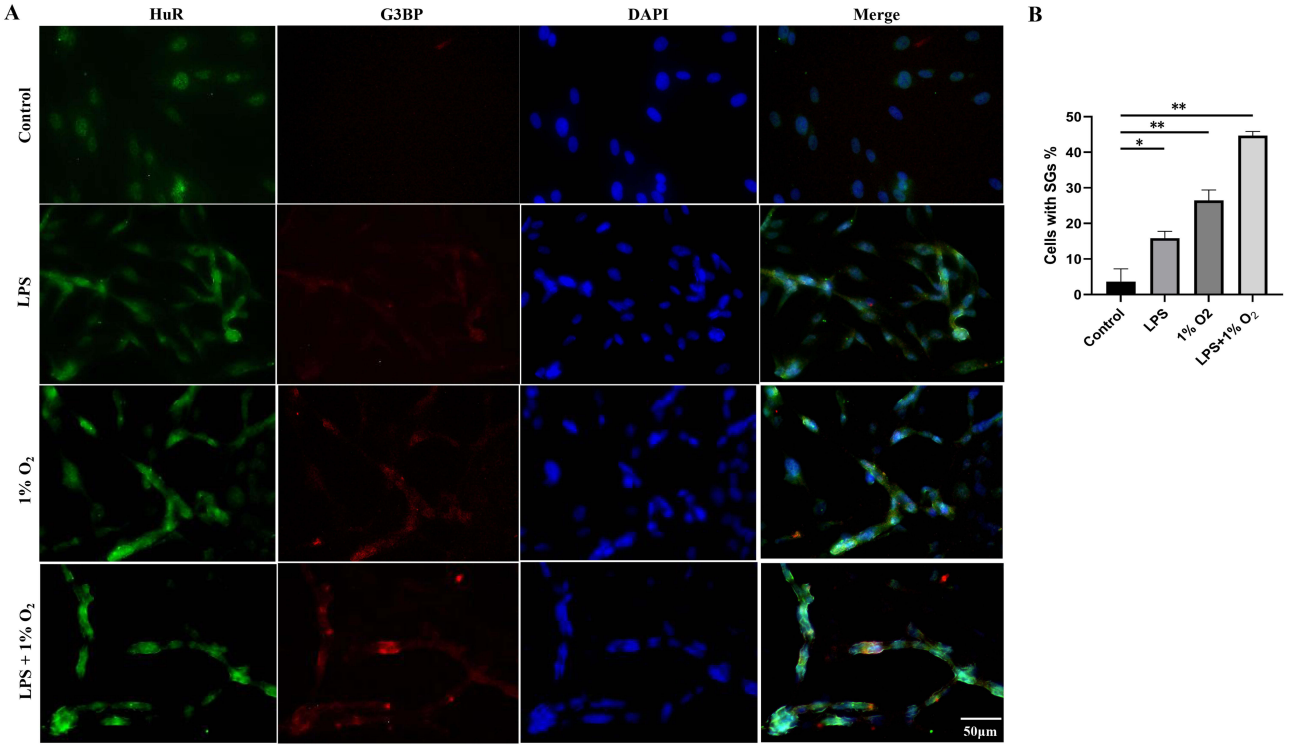

Figure 4 Aggregation of SGs in hGFs under *P. gingivalis*-LPS or 1% O_2 stimulation.(**A**) Immunofluorescent staining of G3BP and HuR and (**B**) the percent of SGs-producing cells in hGFs treated with *P. gingivalis*-LPS (1 μg/mL) or 1% O_2 for 24 h. Scale bar 50 μm. **P*<0.05, ***P*<0.01 vs Control. Data are representative of three independent experiments.

https://doi.org/10.2147/JIR.S523799

PKR-p-eIF2α and 4EBP1 Participate in the P. gingivalis-LPS and 1% O_2 Induced SGs Aggregation in hGFs

Phosphorylation of eIF2α and hypophosphorylation of 4EBP1 are associated with SGs formation under various stress conditions. We further examined p-eIF2α and 4EBP1 protein levels in hGFs after *P. gingivalis*-LPS or 1% O_2 stimulation and found that *P. gingivalis*-LPS or 1% O_2 stimulation increased eIF2α phosphorylation and decreased 4EBP1 phosphorylation, and the combination of *P. gingivalis*-LPS and 1% O_2 treatment was more significant (Figure 5A). Consistently, we found a similar phenomenon in PI gingival tissues, with increased eIF2α phosphorylation and decreased 4EBP1 phosphorylation levels compared to those in normal gingival tissues (Figure 5B).

To further explore the mechanism of SGs formation, we chose *P. gingivalis*-LPS combined with 1% O_2 as the stress condition. We knocked down eIF2α kinase and 4EBP1 using specific siRNAs. siRNA effectively knocked down *PERK, PKR, HRI, GCN2*, and *4EBP1* (Figure 5C). Western blot analysis showed that *PKR* knockdown markedly impaired eIF2α phosphorylation triggered by *P. gingivalis*-LPS and 1% O_2 co-treatment, but not *HRI, PERK*, or *GCN2*, compared to control siRNA, suggesting that PKR kinase plays a specific role in the phosphorylation of eIF2α under *P. gingivalis*-LPS and 1% O_2 stimulation (Figure 5D). We further explored the effect of PKR or 4EBP1 knockdown on SGs aggregation stimulated by *P. gingivalis*-LPS and 1% O_2 co-treatment, using an immunofluorescence assay. As shown in Figure 6A and B, knockdown of PKR or 4EBP1 significantly reduced the number of HuR^+ SGs induced by *P. gingivalis*-LPS and 1% O_2 co-treatment, respectively, suggesting that both PKR-p-eIF2α and 4EBP1 participate in SG aggregation induced by *P. gingivalis*-LPS and 1% O_2.

Inhibition of SGs Formation Promotes the Expression of Inflammatory Factors in hGFs Stimulated by P. gingivalis-LPS and 1% O_2

To further investigate the role of SGs formed in hGFs, we examined changes in the expression of TNF-α and IL-1β after knockdown of PKR or 4EBP1. qPCR results showed that knockdown of PKR or 4EBP1 significantly enhanced the

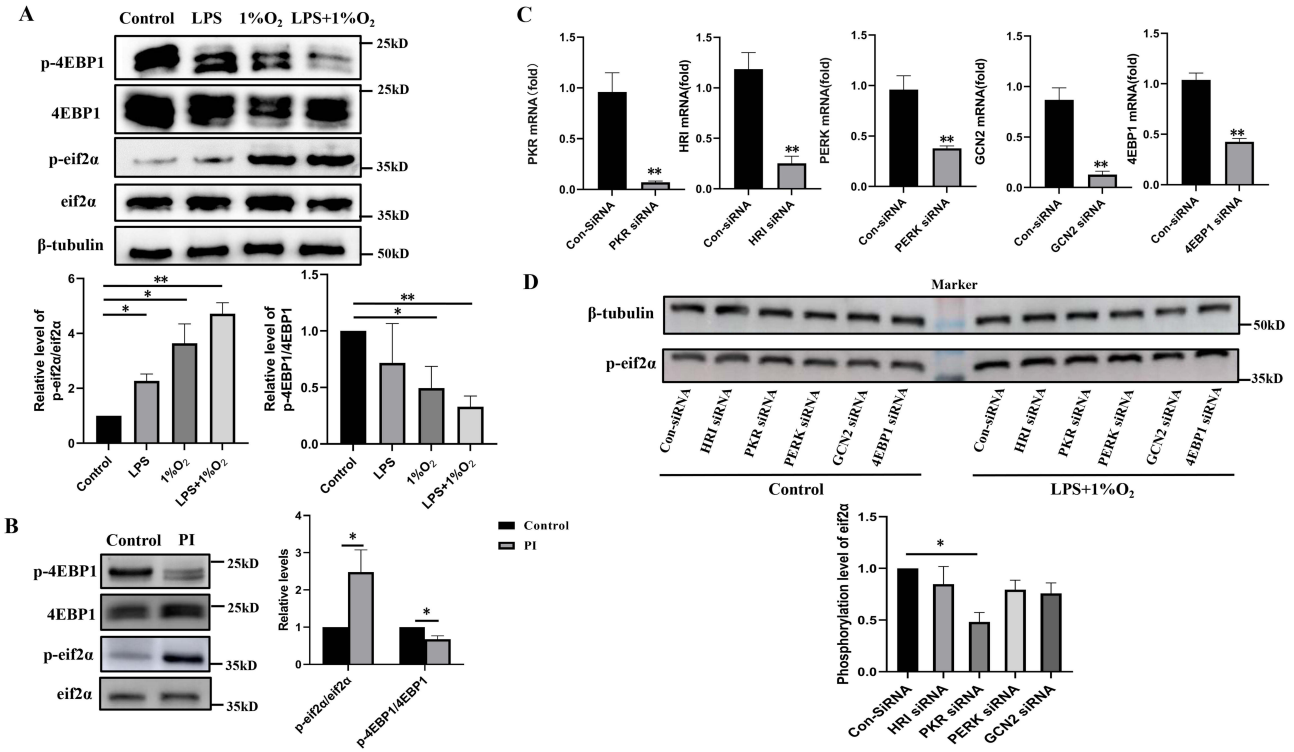

Figure 5 *P. gingivalis*-LPS or 1% O_2 induce PKR-p-eIF2α pathway activation and 4EBP1 hypophosphorylation in stressed hGFs. (**A**) Western blot analysis of whole-cell extracts from hGFs treated with *P. gingivalis*-LPS (1 μg/mL) or 1% O_2 for 24 h. (**B**) Western blot analysis of the gingival tissue (n=6). (**C**) qPCR analysis of eIF2α kinase and 4EBP1 in hGFs transfected with indicated siRNAs for 24 h, respectively. (**D**) hGFs were treated with *P. gingivalis*-LPS (1 μg/mL) combined with 1% O_2 for another 24 h after transfection and Western blot analysis of p-eIF2α was performed. *P<0.05, **P<0.01 vs Control. Data are representative of three independent experiments.

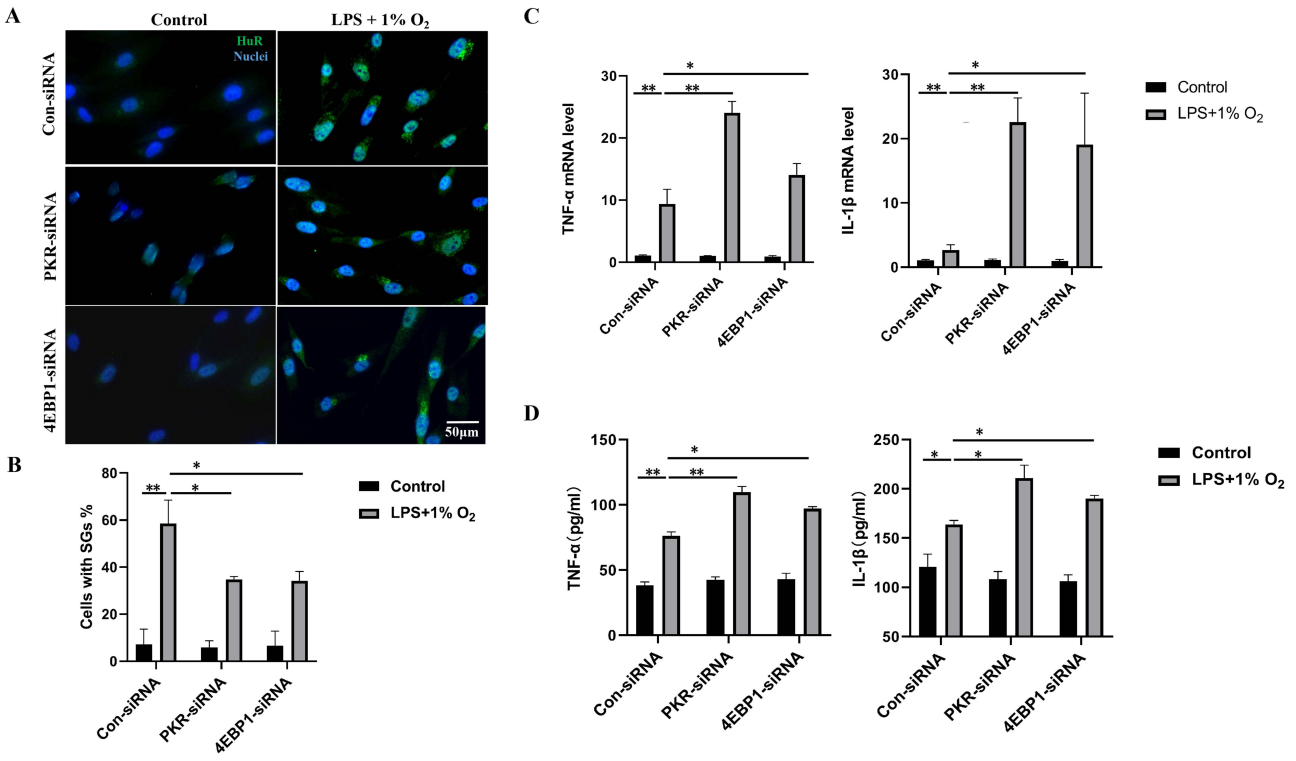

Figure 6 PKR or 4EBP1 knockdown inhibit SGs aggregation and enhance inflammatory response in hGFs stimulated by *P. gingivalis*-LPS and 1% O_2 co-treatment. hGFs were treated with *P. gingivalis*-LPS (1 μg/mL) combined with 1% O_2 for another 24 h after transfection. (**A**) Immunofluorescence staining of HuR and (**B**) the percentage of HuR^+ SG-producing cells in hGFs. Green: HuR, Blue: DAPI. Scale bar 50 μm. (**C**) qPCR analysis of TNF-α and IL-1β expression in hGFs. (**D**) ELISA measurement of TNF-α and IL-1β levels in the supernatant produced by hGFs. **P*<0.05, ***P*<0.01. Data are representative of three independent experiments.

expression of TNF-α and IL-1β in hGFs induced by *P. gingivalis*-LPS and 1% O_2 (Figure 6C). Similar results were obtained using ELISA for changes in TNF-α and IL-1β levels in the culture supernatants of hGFs (Figure 6D). These results show that SGs formation in hGFs induced by *P. gingivalis*-LPS and 1% O_2 can inhibit the inflammatory response. In order to explore the mechanism of SGs formation inhibiting inflammation, we investigated whether this effect may be due to SGs recruiting key inflammatory signaling proteins. Under various pressures, the insoluble parts of many cells are rich in SGs components.[24] We extracted soluble and insoluble fractions from hGFs separately. Western blot analysis showed that compared with untreated hGFs, the insoluble fraction of hGFs treated with *P. gingivalis*-LPS and 1% O_2 was more enriched in SGs marker protein HuR (Figure S1A). In addition, a large proportion of TNF-α receptor-associated factor 2 (TRAF2), a signaling molecule that plays a key role in activation of NF-κB through TNF-α, was also enriched in the insoluble fraction upon *P. gingivalis*-LPS and 1% O_2 treatment (Figure S1A). Immunofluorescence analysis also showed that TRAF2 was recruited into SGs (Figure S1B). Together, these results suggest that *P. gingivalis*-LPS and 1% O_2 can lead to TRAF2 sequestration into SGs and subsequent blockade of TNF-α-mediated NF-κB proinflammatory signaling, one way by which SGs impair the inflammatory process.

Discussion

PI is a major risk factor that affects implant prognosis. The present study showed obvious SGs aggregation in the gingiva of PI patients. In addition, hypoxia and inflammation successfully induced SG formation in hGFs via the PKR-p-eIF2α and 4EBP1 pathways. Interference of SGs formation by PKR or 4EBP1 siRNA significantly increased the production of inflammatory mediators in hGFs. These findings demonstrate that SGs exert a protective effect against damaging pro-inflammatory responses in PI, and may provide a reliable new regulatory mechanism under inflammation and hypoxia for the persistence of PI.

PI gingival tissues exhibit higher inflammation and lower fibroblast counts, accompanied by increased hypoxia and inflammation, compared to healthy gingival tissues.[10] In our study, we also found disruption of collagen fiber bundles in the gingiva of patients with PI, with a reduced number of fibroblasts and dilated capillaries. SGs formation is associated with stress-related and inflammatory diseases such as mucositis, preeclampsia, and cancer.[25–27] SGs formation in stressed cells requires an interaction network between HuR and G3BP.[15] Here, we found increased HuR and G3BP protein levels in the gingiva of PI and detected the $HuR^{+}G3BP^{+}$ SGs structure in PI. The oral bacterial community consists of facultative anaerobic bacteria, as the oxygen tension in the oral cavity is approximately 12–14%, and the oxygen tension in the periodontal pocket is even lower, approximately 1–2%.[28] We then treated hGFs with 1% O_2 or *P. gingivalis*-LPS, a condition phenotype of the chronic inflammatory environment during PI, and found increased HuR and G3BP protein levels and detected the $HuR^{+}G3BP^{+}$ SGs structure, suggesting that *P. gingivalis*-LPS or 1% O_2 treatment alone could induce SGs assembly in hGFs, and that the combination of *P. gingivalis*-LPS and 1% O_2 treatment was more significant. Consistent with our results, Wang et al found that LPS challenge of cardiomyocytes stimulated eIF2α phosphorylation and induced SGs formation.[21] In a study by Knowles et al, *P. gingivalis*-LPS alone failed to induce SGs in squamous oral epithelial cell carcinoma cells. In addition, *P. gingivalis*-LPS did not alter translational repression or eIF2α phosphorylation induced by oxidative stress.[29] These differential responses may be cell type-specific, and oral squamous cell carcinoma epithelial cell lines were less sensitive to LPS stimulation than the primary hGFs used in our study.

Different stresses induce SGs formation triggered by the classical p-eIF2α pathway and/or arrest of translational pre-initiation complexes.[30,31] Translation repressor protein 4EBP1 inhibits cap-dependent translation by binding to eIF4E.[16] In our study, we demonstrated that *P. gingivalis*-LPS and 1% O_2 induced SGs formation in hGFs via PKR-p-eIF2α and 4EBP1 pathways. Inhibition of the PKR-p-eIF2α pathway or 4EBP1 pathway by PKR siRNA or 4EBP1 siRNA significantly reduced SGs assembly. In an experimental periodontitis model, PKR was upregulated and phosphorylated by LPS treatment in osteoclasts, and PKR inhibition suppressed LPS-induced osteoclast formation and NF-κB activation.[32] Here, we found that knockdown of PKR or 4EBP1 obviously enhanced the expression of TNF-α and IL-1β in hGFs induced by *P. gingivalis*-LPS and 1% O_2 treatment, suggesting that SGs formation plays a protective role against the damage induced by *P. gingivalis*-LPS and 1% O_2. SGs formation occurs prior to the intracellular inflammatory response and recruits core signaling proteins as upstream signaling hubs.[33] When specific proteins are sequestered in SGs, their confinement in a negative orientation has cytoprotective effects and vice versa. For example, sequestration of TRAF2 into SGs breaks the positive feedback loop of the pro-inflammatory response through NF-κB and TNF-α.[34] Here, we also found TRAF2 was enriched in the insoluble fraction and recruited into SGs upon *P. gingivalis*-LPS and 1% O_2 treatment. However, the effects of SGs remain controversial. SGs formation initially contributes to cell survival under stress, whereas long-term SGs can promote various diseases.[35–37]

SGs have complex components and dynamic functions, which are difficult to purify in vitro.[38] So far, there is still no effective biochemical method to isolate pure SGs from cells. Although the fractionation method we used here is rough, it represents a simplified and consistent approach to enriching SG components. The limitation of our study is that the impact of SGs depolymerization or protein–protein interactions in SGs has not been studied. Characterization of the components and protein dynamics of SGs in hGFs may promote targeted therapy for PI. In addition, in vivo studies using an animal model of PI[39] should be performed to validate our findings.

Conclusion

In conclusion, our study demonstrated SGs aggregation in PI gingiva. Hypoxia and *P. gingivalis*-LPS can induce SGs assembly in hGFs via PKR-p-eIF2α and 4EBP1 pathways. SGs in hGFs exert a protective effect against hypoxia and *P. gingivalis*-LPS-induced inflammatory responses. The formation of SGs plays a role in balancing pro- and anti-inflammatory responses, and thus provides a new approach for protecting against destructive inflammatory responses.

Data Sharing Statement

The datasets used and/or analyzed during the present study are available from the corresponding author upon reasonable request.

Ethics Statement

This study was approved by the Institutional Review Board (IRB) of the Affiliated Hospital of Qingdao University (IRB No. QYFYWZLL29422). All participants provided informed consent.

Funding

This research was supported by the Application and Basic Research Project of Qingdao West Coast Area (2020-49), the Science and Technology Program of Shinan District of Qingdao (2023-2-005-YY), and the Clinical Medicine + X Research Project of the Affiliated Hospital of Qingdao University (QDFY+X2023119).

Disclosure

Shuang Li and Chunling Ma are co-first authors for this study. Na Bai and Zhiyuan Li are co-correspondence authors for this study. The authors declare no conflicts of interest in this work.

References

1. Caton JG, Armitage G, Berglundh T, et al. A new classification scheme for periodontal and peri-implant diseases and conditions - Introduction and key changes from the 1999 classification. *J Clin Periodontol*. 2018;45:s1–s8. doi:10.1111/jcpe.12935
2. Berglundh T, Mombelli A, Schwarz F, Derks J. Etiology, pathogenesis and treatment of peri-implantitis: a European perspective. *Periodontol 2000*. 2024;1–36 doi:10.1111/prd.12549.
3. Llopis-Grimalt MA, Munar-Bestard M, Ramis-Munar G, et al. Nanostructured implant-tissue interface assessment using a three-dimensional gingival tissue equivalent. *ACS Omega*. 2024;9:30534–30543. doi:10.1021/acsomega.4c02253
4. Chmielewski M, Pilloni A. Current molecular, cellular and genetic aspects of peri-implantitis disease: a narrative review. *Dent J*. 2023;11:134. doi:10.3390/dj11050134
5. Irshad M, Scheres N, Anssari Moin D, et al. Cytokine and matrix metalloproteinase expression in fibroblasts from peri-implantitis lesions in response to viable porphyromonas gingivalis. *J Periodontal Res*. 2013;48:647–656. doi:10.1111/jre.12051
6. Liu J, Zeng J, Wang X, Zheng M, Luan Q. P53 mediates lipopolysaccharide-induced inflammation in human gingival fibroblasts. *J Periodontol*. 2018;89:1142–1151. doi:10.1002/JPER.18-0026
7. de Araújo MF, Etchebehere RM, de Melo MLR, et al. Analysis of CD15, CD57 and HIF-1α in biopsies of patients with peri-implantitis. *Pathol Res Pract*. 2017;213:1097–1101. doi:10.1016/j.prp.2017.07.020
8. Gölz L, Memmert S, Rath-Deschner B, et al. Hypoxia and P. gingivalis synergistically induce HIF-1 and NF-κB activation in PDL cells and periodontal diseases. *Mediators Inflamm*. 2015;2015:438085. doi:10.1155/2015/438085
9. Ivanovski S, Lee R. Comparison of peri-implant and periodontal marginal soft tissues in health and disease. *Periodontology*. 2018;76:116–130. doi:10.1111/prd.12150
10. Karatas O, Balci Yuce H, Taskan MM, Gevrek F, Lafci E, Kasap H. Histological evaluation of peri-implant mucosal and gingival tissues in peri-implantitis, peri-implant mucositis and periodontitis patients: a cross-sectional clinical study. *Acta Odontol Scand*. 2020;78:241–249. doi:10.1080/00016357.2019.1691256
11. Riggs CL, Kedersha N, Ivanov P, Anderson P. Mammalian stress granules and P bodies at a glance. *J Cell Sci*. 2020;133:jcs242487. doi:10.1242/jcs.242487
12. Emara MM, Fujimura K, Sciaranghella D, Ivanova V, Ivanov P, Anderson P. Hydrogen peroxide induces stress granule formation independent of eIF2α phosphorylation. *Biochem Biophys Res Commun*. 2012;423:763–769. doi:10.1016/j.bbrc.2012.06.033
13. Buchan JR, Parker R. Eukaryotic stress granules: the ins and outs of translation. *MolCell*. 2009;36:932–941. doi:10.1016/j.molcel.2009.11.020
14. Li W, Wang Y. Stress granules: potential therapeutic targets for infectious and inflammatory diseases. *Front Immunol*. 2023;14:1145346. doi:10.3389/fimmu.2023.1145346
15. Anderson P, Kedersha N. Stress granules: the Tao of RNA triage. *Trends Biochem Sci*. 2008;33:141–150. doi:10.1016/j.tibs.2007.12.003
16. Fujimura K, Sasaki AT, Anderson P. Selenite targets eIF4E-binding protein-1 to inhibit translation initiation and induce the assembly of non-canonical stress granules. *Nucleic Acids Res*. 2012;40:8099–8110. doi:10.1093/nar/gks566
17. Reineke LC, Dougherty JD, Pierre P, Lloyd RE. Large G3BP-induced granules trigger eIF2α phosphorylation. *Mol Biol Cell*. 2012;23:3499–3510. doi:10.1091/mbc.e12-05-0385
18. Fournier MJ, Coudert L, Mellaoui S, et al. Inactivation of the mTORC1-eukaryotic translation initiation factor 4E pathway alters stress granule formation. *Mol Cell Biol*. 2013;33:2285–2301. doi:10.1128/MCB.01517-12
19. Jiang H-Y, Gu -W-W, Gan J, et al. MNSFβ promotes LPS-induced TNFα expression by increasing the localization of RC3H1 to stress granules, and the interfering peptide HEPN2 reduces TNFα production by disrupting the MNSFβ–RC3H1 interaction in macrophages. *Int Immunopharmacol*. 2024;142:113053. doi:10.1016/j.intimp.2024.113053
20. Qi X, Zhao R, Yao X, et al. Getah virus Nsp3 binds G3BP to block formation of bona fide stress granules. *Int J Biol Macromol*. 2024;279:135274. doi:10.1016/j.ijbiomac.2024.135274
21. Wang Y, Liu R, Wu K, et al. Stress granule activation attenuates lipopolysaccharide-induced cardiomyocyte dysfunction. *BMC Cardiovasc Disord*. 2023;23:277. doi:10.1186/s12872-023-03281-0
22. Dong T, Zhao F, Wang M, et al. G3BP1/2-Targeting PROTAC disrupts stress granules dependent ATF4 migracytosis as cancer therapy. *J Am Chem Soc*. 2024;147:446–461. doi:10.1021/jacs.4c11146
23. Berglundh T, Armitage G, Araujo MG, et al. Peri-implant diseases and conditions: consensus report of workgroup 4 of the 2017 world workshop on the classification of periodontal and peri-implant diseases and conditions. *J Clin Periodontol*. 2018;45:s286–s291. doi:10.1111/jcpe.12957

24. Omer A, Patel D, Lian XJ, et al. Stress granules counteract senescence by sequestration of PAI-1. *EMBO Rep*. 2018;19:e44722. doi:10.15252/embr.201744722
25. Ma C, Lv Q, Ma L, Xing B, Li Y. $CoCl_2$-mimicked hypoxia induces the assembly of stress granules in trophoblast cells Via eIF2α Phosphorylation-dependent and - independent pathways. *Curr Mol Med*. 2024;24:1291–1300. doi:10.2174/1566524023666230913111300
26. Li T, Zeng Z, Fan C, Xiong W. Role of stress granules in tumorigenesis and cancer therapy. *Biochim Biophys Acta Rev Cancer*. 2023;1878:189006. doi:10.1016/j.bbcan.2023.189006
27. Hu S, Claud EC, Musch MW, Chang EB. Stress granule formation mediates the inhibition of colonic Hsp70 translation by interferon-gamma and tumor necrosis factor-alpha. *Am J Physiol Gastrointest Liver Physiol*. 2010;298:481–492. doi:10.1152/ajpgi.00234.2009
28. Grant MM, Kolamunne RT, Lock FE, Matthews JB, Chapple IL, Griffiths HR. Oxygen tension modulates the cytokine response of oral epithelium to periodontal bacteria. *J Clin Periodontol*. 2010;37:1039–1048. doi:10.1111/j.1600-051X.2010.01622.x
29. Knowles AA, Campbell SG, Cross NA, Stafford P. Dysregulation of stress-induced translational control by porphyromonas gingivalis in host cells. *Microorganisms*. 2023;11:606. doi:10.3390/microorganisms11030606
30. Fritzlar S, Aktepe TE, Chao YW, et al. Mouse norovirus infection arrests host cell translation uncoupled from the stress granule-PKR-eIF2α Axis. *mBio*. 2019;10:e00960–19. doi:10.1128/mBio.00960-19
31. Wang T, Tian X, Kim HB, et al. Intracellular energy controls dynamics of stress-induced ribonucleoprotein granules. *Nat Commun*. 2022;13:5584. doi:10.1038/s41467-022-33079-1
32. Teramachi J, Inagaki Y, Shinohara H, et al. PKR regulates LPS-induced osteoclast formation and bone destruction in vitro and in vivo. *Oral Dis*. 2017;23:181–188. doi:10.1111/odi.12592
33. Kedersha N, Ivanov P, Anderson P. Stress granules and cell signaling: more than just a passing phase? *Trends Biochem Sci*. 2013;38:494–506. doi:10.1016/j.tibs.2013.07.004
34. Kim WJ, Back SH, Kim V, Ryu I, Jang SK. Sequestration of TRAF2 into stress granules interrupts tumor necrosis factor signaling under stress conditions. *Mol Cell Biol*. 2005;25:2450–2462. doi:10.1128/MCB.25.6.2450-2462.2005
35. Xu J, Hu C, Chen S, et al. Neuregulin-1 protects mouse cerebellum against oxidative stress and neuroinflammation. *Brain Res*. 2017;1670:32–43. doi:10.1016/j.brainres.2017.06.012
36. Wang F, Li J, Fan S, Jin Z, Huang C. Targeting stress granules: a novel therapeutic strategy for human diseases. *Pharmacol Res*. 2020;161:105143. doi:10.1016/j.phrs.2020.105143
37. Mateju D, Chao JA. Stress granules: regulators or by-products? *FEBS J*. 2022;289:363–373. doi:10.1111/febs.15821
38. Buchan JR, Yoon JH, Parker R. Stress-specific composition, assembly and kinetics of stress granules in Saccharomyces cerevisiae. *J Cell Sci*. 2011;124:228–239. doi:10.1242/jcs.078444
39. Hiyari S, Naghibi A, Wong R, et al. Susceptibility of different mouse strains to peri-implantitis. *J Periodontal Res*. 2018;53:107–116. doi:10.1111/jre.12493